Angular and Distance Dependence of the Magnetic Properties of Oxo-Bridged Iron(III) Dimers

Högni Weihe* and Hans U. Güdel*

Contribution from the Department of Chemistry and Biochemistry, University of Bern, Freiestrasse 3, CH-3000 Bern 9, Switzerland

Received January 30, 1997[⊗]

Abstract: The magnetic properties of oxo-bridged oxo-(carboxylato)-bridged and oxo-bis(carboxylato)-bridged iron(III) dimers are found to depend on the iron−(μ-O) distance as well as on the iron−(μ-O)−iron angle. With an angular and radial overlap model we account for both these dependencies. The use of an angular overlap model allows us to separate the σ donor properties of oxide as a ligand into the sσ and pσ contributions.

1. Introduction

The magnetic properties of exchange coupled dinuclear complexes of transition metal ions are known to depend on the particular metal ions, the chemical nature of the bridging ligands, and the bridging geometries.[1] Both bridging angles and bridging ligand−metal distances are of importance. On the basis of empirical magneto-structural correlations, the temperature dependence of the magnetic susceptibility of new compounds can be used for a prediction of the relevant structural parameters. The dimeric structure of copper(II) acetate was predicted on the basis of electron paramagnetic resonance and magneto-chemical studies.[2] A linear correlation between the Cu−O(H)−Cu angle and the magnetic interaction in dihydroxo-bridged copper(II) dimers has been empirically established and theoretically rationalized.[3] The magnetic properties of dihydroxo-bridged chromium(III) dimers were found to depend on the Cr−O(H) distance, the Cr−O(H)−Cr angle, and the position of the H atom on the hydroxide group relative to the Cr−O−Cr plane.[4]

Several natural enzymatic systems contain polynuclear iron centers. The fact that the oxidized form of hemerythrin was shown to contain the μ-oxo-bis(μ-carboxylato)diiron(III) unit[5] has resulted in a renaissance of the Fe−O−Fe unit in the chemical arena. Recently, it was also shown, that ribonucleotide reductase of *E. coli* contains a ferric dimer containing an oxo bridge supported by one carboxylato bridge.[6] Several model systems have been synthesized in order to understand the chemistry,[7] optical properties,[8] and the magnetic properties of this unit. In this paper we focus on the magnetic properties of the μ-oxo diferric unit.

The relevant structural and magnetic properties of 32 model compounds containing the Fe−O−Fe unit are collected in Table 1. In this study we include structurally and magnetically characterized mono-, doubly-, and triply-bridged diiron(III)

complexes from the literature which have only one structural and compositional feature in common, namely the μ-oxo bridge. The additional one or two supporting bridging ligands are in all cases carboxylates or phosphates. They are assumed to play a negligible role as exchange pathways compared to the bridging oxide.[9] The magnetic properties are given in terms of J and g, which are the parameters of the effective Hamiltonian

$$\hat{H} = J\hat{\mathbf{S}}_1 \cdot \hat{\mathbf{S}}_2 + g\mu_B \mathbf{B}(\hat{\mathbf{S}}_1 + \hat{\mathbf{S}}_2) \qquad (1)$$

with $S_1 = {}^5/_2 = S_2$. The eigenvalues of eq 1 are fitted to the magnetic susceptibility as a function of temperature to obtain the adjustable parameters J and g. The J values lie in the interval 160−265 cm^{-1}, and the g values are, with few exceptions, all close to the free electron g value $g_e = 2.0023$. The Fe−O−Fe angle ϕ varies from 113.8° to 180°. The Fe−O distances r_1 and r_2 range from 1.747 to 1.839 Å. The raw experimental data presented in Table 1 were analysed for correlation and association between J and r and between J and ϕ with several standard statistical methods.[32] Both correlations were found negative, and the strength of the (J,r) correlation is 2−3 times stronger than the (J,ϕ) correlation.

There have been several empirical, semiempirical, and theoretical attempts to correlate the experimentally determined J values of oxo-bridged iron(III) dimers to the bridging geometry. This has led to some conflicting conclusions and the situation is presently not clear. Gerloch *et al.*[10] expected a rapid decrease of J upon decreasing the Fe−O−Fe angle ϕ from 180°. Holm *et al.*[11] observed a slow decrease of J as ϕ was decreased. It has also been concluded that there was no correlation of J with the bridging angle.[12,39] Gorun and Lippard[14] thus ignored the angular dependence and included only the Fe−O distance in their ansatz

$$J = A\mathrm{e}^{-BP} \qquad (2)$$

with $A = 8.763 \times 10^{11}$ cm^{-1} and $B = 12.663$ Å^{-1}. P is half the shortest superexchange pathway between the two ferric ions.

[⊗] Abstract published in *Advance ACS Abstracts,* July 1, 1997.

(1) Willet, R. D.; Gatteschi, D.; Kahn, O. *Magneto-Structural Correlations in Exchange Coupled Systems*; Proceeding of the NATO ASI; D. Reidel Publishing Company: Dordrecht, Holland, 1985.

(2) Bleaney, B.; Bowers, K. D. *Proc. R. Soc.* **1952,** *A214,* 451. See also: Bleaney, B.; Bowers, K. D. *Philos. Mag.* **1952,** *43,* 372.

(3) Willet, R. D. in ref 1.

(4) Glerup, J.; Hodgson, D. J.; Pedersen, E. *Acta Chem. Scand.* **1983,** *A37,* 161.

(5) Stenkamp, R. E.; Sieker, L. C.; Jensen, L. H. *J. Am. Chem. Soc.* **1984,** *106,* 618.

(6) Norlund, P.; Sjöberg, B-M.; Eklund, H. *Nature* **1990,** *345,* 593.

(7) Hazell, A.; Jensen, K. B.; McKenzie, C. J.; Toftlund, H. *Inorg. Chem.* **1994,** *33,* 3127.

(8) Spool, A.; Williams, I. D.; Lippard, S. J. *Inorg. Chem.* **1985,** *24,* 2156.

(9) Norman, R. E.; Yan, S.; Que, L.; Backes, G.; Ling, J.; Sanders-Loehr, J.; Zhang, J. H.; O'Connor, C. J. *J. Am. Chem. Soc.* **1990,** *112,* 1554.

(10) Gerloch, M.; Towl, A. D. C. *J. Chem. Soc. A* **1969,** 2850.

(11) Mukherjee, R. N.; Stack, T. D. P.; Holm, R. H. *J. Am. Chem. Soc.* **1988,** *110,* 1850.

(12) Mabbs, F. E.; McLachlan, V. N.; McFadden, D.; McPhail, A. T. *J. Chem. Soc., Dalton Trans.* **1973,** 2016.

(13) Turowski, P. N.; Armstrong, W. H.; Roth, M. E.; Lippard, S. J. *J. Am. Chem. Soc.* **1990,** *112,* 681.

(14) Gorun, S. M.; Lippard, S. J. *Inorg. Chem.* **1991,** *30,* 1625.

Table 1.   Magnetostructural Correlation of 32 μ-Oxo-Bridged Iron(III) Dimers from the Literature[a]

compound[b]	CN	J/cm^{-1}	g	r_1, r_2 (Å)	ϕ/deg	ref
[(TPC)$_2$Fe$_2$(O)]·4CHCl$_3$	5	265[c]	2.00	1.747(5), 1.763(5)	180(0)	33
[(Cl-C$_7$H$_2$NO$_4$)$_2$(H$_2$O)$_4$Fe$_2$(O)]·4H$_2$O	6	214[d]	2.00	1.772(3), 1.773(2)	180(0)	30
[(TPP)$_2$Fe$_2$(O)]	5	258[c]	2.00	1.759(1)	176.1(2)	33
[(tpa)$_2$Cl$_2$Fe$_2$(O)](ClO$_4$)$_2$	6	232	2.03	1.785(1)	174.7(5)	7
[(3-^{t}Bu-saltmen)$_2$Fe$_2$(O)]	5	200[d]	2.00	1.774(4), 1.783(4)	173.5(3)	11
(enH$_2$)[(HEDTA)$_2$Fe$_2$(O)]·6H$_2$O	6	172	2.0	1.80(1), 1.79(1)	165.0(8)	34
[(FF)$_2$Fe$_2$(O)]·H$_2$O·2toluene	5	215	2.00	1.774(6), 1.800(6)	161.1(4)	35
[(phen)$_4$(H$_2$O)$_2$Fe$_2$(O)](NO$_3$)$_4$·5H$_2$O	6	220		1.787(5), 1.783(5)	155.1(4)	36
[(2-Me-quin)$_2$Fe$_2$(O)]	5	160	2.00	1.801(11)	151.6(7)	12
[(salen)$_2$Fe$_2$(O)]	5	184[d]	2.009	1.78(1)	144.6(6)	11
[(cbpN)$_2$Fe$_2$(O)]·o-xylene	6	160		1.807(3), 1.804(3)	144.5(2)	37
[(salen)$_2$Fe$_2$(O)]·CH$_2$Cl$_2$	5	174	2.00	1.791(9), 1.797(9)	142.4(5)	38
[(tpa)$_2$Fe$_2$(O)(phtal)](ClO$_4$)$_2$·MeOH·H$_2$O	6	220	2.00	1.785(5), 1.799(5)	143.4(3)	39
[(tpa)$_2$Fe$_2$(O)(H$_3$O$_2$)](ClO$_4$)$_3$	6	194	1.90	1.780(6), 1.839(6)	138.9(4)	7
[(tpa)$_2$Fe$_2$(O)(O$_2$P(OC$_6$H$_5$)$_2$)](ClO$_4$)$_3$·CH$_3$COCH$_3$	6	202	2.04	1.815(5), 1.779(3)	138.1(2)	9
[(tpa)$_2$Fe$_2$(O)(malH)](ClO$_4$)$_3$·2CH$_3$COCH$_3$	6	240	2.03	1.779(5), 1.808(6)	131.0(3)	39
[(tpa)$_2$Fe$_2$(O)(O$_2$CC$_6$H$_5$)](ClO$_4$)$_3$	6	237	2.06	1.776(4), 1.804(5)	129.7(3)	9
[(tpa)$_2$Fe$_2$(O)(acO)](ClO$_4$)$_3$·H$_2$O·CH$_3$COCH$_3$	6	228	2.04	1.790(5), 1.800(4)	129.2(2)	9
[L$_2$Fe$_2$(O)(CO$_3$)](ClO$_4$)$_2$·2H$_2$O	6	204	2.01	1.800(5), 1.807(5)	126.1(3)	40
[(tpa)$_2$Fe$_2$(O)(CO$_3$)](ClO$_4$)$_2$·2MeOH	6	217	2.02	1.784(5), 1.817(5)	125.4(3)	39
[(HB(pz)$_3$)$_2$Fe$_2$(O)(O$_2$P(OC$_6$H$_5$)$_2$)$_2$)]·CHCl$_3$	6	195		1.807(3), 1.808(3)	134.7(2)	13
[(HB(pz)$_3$)$_2$Fe$_2$(O)(O$_2$P(C$_6$H$_5$)$_2$)$_2$)]·CH$_2$Cl$_2$·CCl$_4$	6	190[c]		1.812(3)	130.6(3)	13
[(BIPhMe)$_2$Cl$_2$Fe$_2$(O)(MPDP)]	6	244	2.00	1.783(5), 1.790(4)	125.9(2)	16
[cpCo((EtO)$_2$PO)$_2$Fe(O)(acO)$_2$]	6	217		1.791(6), 1.799(6)	124.4(4)	41
[(4,4′-Me$_2$bpy)$_2$Cl$_2$Fe$_2$(O)(MPDP)]	6	238	2.00	1.771(3), 1.774(3)	124.0(2)	16
[(bpy)$_2$Cl$_2$Fe$_2$(O)(acO)$_2$]·CH$_3$CN	6	264	1.90	1.783(3), 1.787(4)	123.9(2)	42
[(HB(pz)$_3$)$_2$Fe$_2$(O)(acO)$_2$]	6	243[d]	2.00	1.780(2), 1.788(2)	123.6(1)	43
[(Me$_3$tacn)$_2$Fe$_2$(O)(PO$_3$(C$_6$H$_5$))$_2$]·NaClO$_4$·2H$_2$O	6	196	2.06	1.817(5)	123.2(3)	44
[(Me$_3$tacn)$_2$Fe$_2$(O)(acO)$_2$](ClO$_4$)$_2$·H$_2$O	6	238[c]	2.00	1.800(3)	119.7(1)	45
[L$_2$Fe$_2$(O)(O$_2$CC$_6$H$_5$)](ClO$_4$)$_2$·2EtOH·0.5Et$_3$NHClO$_4$	6	234	2.00	1.777(5), 1.802(6)	118.7(3)	46
[L$_2$Fe$_2$(O)((CH$_3$)$_3$CCO$_2$)$_2$](ClO$_4$)$_2$	6	232	2.04	1.803(6)	117.0(6)	47
[(Me$_3$tacn)$_2$Fe$_2$(O)(CO$_3$)$_2$]·4.25H$_2$O	6	182	1.999	1.813(7), 1.826(8)	113.8(4)	48

[a] The first column lists formulas for the compounds included in this study. acO stands for acetate. The second column gives the coordination number (CN) of each iron center. The third and fourth columns list the J and g values derived from a fit to the temperature dependence of the magnetic susceptibility, respectively. g values differing from 2.00 were varied in the fittings of the magnetic susceptibility data. The fifth and sixth columns contain the relevant structural data. [b] TPC = 5,10,15,20-tetraphenylporphyrinato, Cl-C$_7$H$_2$NO$_4$ = 4-chloro-2,6-pyridinedicarboxylate. TPP = 7.8-dihydro-5,10,15,20-tetraphenylporphyrinato. tpa = tris(2-pyridylmethyl)amine. H$_2$(3-Bu-salt-men) = 2,3-dimethyl-2,3-bis(3-butylsalicyl-idenamino)butane. en = ethylenediamine. HEDTA = N-hydroxyethylethylenediaminetriacetato. FF = N,N'-bis(5-(o-phenyl)-10,15,20-triphenyl-porphyrin) urea. phen = 1,10-phenantroline. 2-Me-quin = 8-hydroxy-2-methylquinolato. salen = 1,2-bis(salicylideneaminato)ethane(2−). cbpN is the pentadentate ligand produced by condensing 1,4,7-triazacyclononane with two units of 2-hydroxy-5-chlorobenzophenone. phtal = phtalate. H$_3$O$_2$ is short for the bridging arrangement HO−H−OH. malH = hydrogen maleate. Me$_3$tacn = 1,4,7-trimethyl-1,4,7-triazacyclononane. HB(pz)$_3$ = hydridotris(pyrazolyl)borate. BIPhMe = bis(1-methylimidazol-2-yl)phenylmethoxymethane. MPDP = m-phenylenedipropionate. cp = cyclopentadienyl. 4,4′-Me$_2$bpy = 4,4′-dimethyl-2,2′-bipyridine. bpy = 2,2′-bipyridine. L = bis(2-benzimidazolylmethyl)amine. L = N,N'-dimethyl-N,N'-bis(2-pyridylmethyl)ethane-1,2-diamine. [c] It was necessary to include a Weiss parameter associated with the paramagnetic impurity in order to get a good fit of the temperature-dependent magnetic susceptibility curve. [d] Several interpretations of the susceptibility data were reported.

With eq 2 they were able to account for J values in widely different types of dimeric and trimeric iron(III) complexes having one oxo bridge, one hydroxo bridge, or one alkoxo bridge and at least one more bridging ligand. However, the physical meaning of the purely empirical parameters A and B in eq 2 remains obscure. Recently it was suggested that J correlates with the longest, rather than the mean Fe−(μ-O) bond length in asymmetric Fe−O−Fe units.[7] And finally, a slight increase of J upon lowering ϕ was found in an *ab initio* study of the related Cl$_3$FeOFeCl$_3^{2-}$ anion.[15]

As a result of this rather confusing situation we decided to analyze these systems, taking into account the structural parameters ϕ, r_1, and r_2 (see Figure 1). Table 1 shows that asymmetric complexes in which $r_1 \neq r_2$ are the rule rather than the exception in these dimers. At first sight there is no empirical correlation between the J value and any of the three parameters. We therefore introduce a physical model that connects J with the structural parameters by a mathematical formula. We thus obtain some physical insight into the important interaction

Figure 1. Definition of the coordinate system distances and angles used in the text. The y_1 and y_2 axes point toward the viewers eye.

pathways. This will allow us to address the question of why J is so seemingly insensitive to changes of ϕ. This question is interesting because the magnetic properties of other oxo-bridged dimers depend dramatically on ϕ.[18] The model we use is a time tested chemically intuitive one, namely the angular overlap model (AOM). We will be able to express J in terms of overlaps between the iron d orbitals and the bridging oxide p and s orbitals. Since such overlaps are both distance and angle dependent, we will be able to take account of r_1, r_2, and ϕ in our semiempirical model. In addition we will be able to separate the sσ and pσ contributions to the AOM parameters and finally make a prediction of J values for new Fe−O−Fe complexes on the basis of their bridging parameters.

(15) Hart, J. R.; Rappe, A. K.; Gorun, S. M.; Upton, T. H. *Inorg. Chem.* **1992**, *31*, 5254.

(16) Beer, R. H.; Tolman, W. B.; Bott, S. G.; Lippard, S. J. *Inorg. Chem.* **1989**, *28*, 4557.

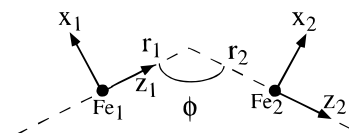(17) Weihe, H.; Güdel, H. U. *Inorg. Chem.*, in press.

(18) Weihe, H.; Güdel, H. U. *Inorg. Chem.* To be submitted for publication.

2. Model and Calculations

The coordinate systems defined on the two Fe centers of the dimer are shown in Figure 1. We assume that the interaction takes place mainly through the bridging oxide ion, *i.e.* we neglect any interaction through the supporting bridging ligand(s) and direct metal—metal interactions. In the following treatment we also neglect the characteristics of the terminal ligands except for their influence on the bridging geometry. This is justified by the fact that *J* is not found to be significantly altered by substituting chloride for a terminal nitrogen donor.[16] Since the relevant oxide orbitals are the filled 1s, 2s, and 2p orbitals, we only need to consider metal orbitals with σ and π symmetry with respect to the Fe—O bonds. These metal orbitals are

$$\theta_i \equiv (d_{z^2})_i \tag{3}$$

and

$$\eta_i \equiv (d_{zx})_i \tag{4}$$

$$\xi_i \equiv (d_{yz})_i \tag{5}$$

respectively. $i = 1$ or 2 numbers the two high-spin ferric ions in the dimer. Considering only kinetic exchange,[19] *i.e.* the second-order effect of virtual electron transfer between metal ions, *J* for an iron(III) dimer can be expressed as

$$J_{model} = \frac{4}{25}\frac{1}{U}(h_{\eta\eta}^2 + h_{\xi\xi}^2 + h_{\theta\theta}^2 + h_{\eta\theta}^2 + h_{\theta\eta}^2) \tag{6}$$

where *U* is the energy of a charge-transfer state,[19] see also ref 17 for details. In eq 6 h_{ab} is the one-electron transfer integral between the a orbital on metal center 1 and the b orbital on metal center 2. It has been shown that the transfer integrals can be expressed in terms of the well-known AOM ligand-field parameters.[20–22] Defining the Fe_1—O and Fe_2—O distances as r_1 and r_2, respectively, and using the procedure described in ref 25 we find the following expressions for the relevant transfer integrals:

$$h_{\eta\eta} = \sqrt{e_{p\pi}(r_1)}\sqrt{e_{p\pi}(r_2)}(-\cos\phi) \tag{7}$$

$$h_{\xi\xi} = \sqrt{e_{p\pi}(r_1)}\sqrt{e_{p\pi}(r_2)} \tag{8}$$

$$h_{\theta\theta} = \sqrt{e_{s\sigma}(r_1)}\sqrt{e_{s\sigma}(r_2)} - \sqrt{e_{p\sigma}(r_1)}\sqrt{e_{p\sigma}(r_2)}(-\cos\phi) \tag{9}$$

$$h_{\eta\theta} = \sqrt{e_{p\pi}(r_1)}\sqrt{e_{p\sigma}(r_2)}(\sin\phi) \tag{10}$$

$$h_{\theta\eta} = \sqrt{e_{p\sigma}(r_1)}\sqrt{e_{p\pi}(r_2)}(\sin\phi) \tag{11}$$

In terms of the well-known Goodenough—Kanamori rules[23] and the old magnetochemical literature,[24] the parameters $h_{\eta\eta}$ and $h_{\xi\xi}$ both correspond to $\pi\pi$ superexchange pathways. $h_{\theta\theta}$ corresponds to a $\sigma\sigma$, $h_{\eta\theta}$ and $h_{\theta\eta}$ to $\pi\sigma$ and $\sigma\pi$ superexchange pathways, respectively. Our expressions are in accordance with ref 22, but there only the situations for $\phi = 90°$ and $\phi = 180°$ were considered. The formalism leading to eqs 7–11 was also applied in ref 21 for dibridged copper(II) dimers. In eqs 7–11 $e_{a\alpha}(r_i)$ is the aα ligand-field parameter in the AOM formulation for the Fe—O bond. The parameters $e_{a\alpha}(r_i)$ are distance dependent, and we separate the *r* dependence as follows

$$\sqrt{e_{a\alpha}(r)} = f(r)\sqrt{e_{a\alpha}} \tag{12}$$

where $f(r)$ is proportional to the overlap $\langle d_\alpha | a\alpha \rangle$ at distance *r*. We use the two trial radial functions[27]

$$f(r) \propto e^{-br} \tag{13}$$

$$f(r) \propto r^{-b} \tag{14}$$

Both radial dependencies eqs 13 and 14 fulfill the requirement, provided $b > 0$, that overlaps decrease with increasing distance between the relevant orbitals. Both functions 13 and 14 have been used in numerous studies of the radial dependence of the *J* parameter.[14,27–29] The results for both radial functions will be presented in the next section.

The value of the quantity *U* in eq 6 is not directly accessible by experiment. Only rough estimates can be made, and we are thus not in a position to determine absolute values of J_{model}. Combining eqs 6, 7–11, and 12 we can write

$$J_{model} = \frac{4}{25}[e_{p\pi}'^2(1 + \cos^2\phi) + (e_{s\sigma}' - e_{p\sigma}'(-\cos\phi))^2 +$$
$$2e_{p\sigma}'e_{p\pi}'(\sin\phi)^2]\, f^2(r_1)\, f^2(r_2)$$
$$= \frac{4}{25}\, G(\phi)\, F(r_1,r_2) \tag{15}$$

where the *U* of eq 6 and a proportionality constant of eq 13 or 14 together with the AOM parameter $e_{a\alpha}$ of eq 7–11 make up the primed parameter $e_{a\alpha}'$. Notice that J_{model} in eq 15 is a product of an angular function $G(\phi)$ and a radial function $F(r_1,r_2)$. This is a result of our assumption that all the relevant overlaps have the same radial dependence, *i.e.* the same numerical value of *b* in eq 13 or 14. From eq 15 we see that our description of the situation directly leads to the implication that *J*, for fixed ϕ, is proportional to the fourth power of the $\langle d_\alpha | a\alpha \rangle$ overlaps. This has been found to be well fulfilled in theoretical studies of the exchange coupling phenomenon.[15,29] Hence

$$J \propto \exp(-4br) \tag{16}$$

or approximately

$$J \propto r^{-4b} \tag{17}$$

in the case of the radial dependencies eq 13 or 14, respectively.

We use eq 15 with ϕ, r_1, and r_2 from Table 1 as input and $e_{s\sigma}'$, $e_{p\sigma}'$, $e_{p\pi}'$, and *b* as adjustable parameters to compute J_{model} for all 32 entries in Table 1. The model parameters are determined by minimizing the function

$$\chi^2 = \sum_{compounds} (J - J_{model})^2 \tag{18}$$

We performed unweighted least-squares fittings only, since the experimental *J* and *g* values are usually not reported with an error bar. It is interesting to note and of relevance here that different analyses of the same susceptibility data can lead to *J* values varying by as much as 21 cm^{-1}.[11,30] This is probably an upper limit for the standard deviation of the experimental *J* values. There is no reason that *g* should deviate much from 2.00.[31] Nevertheless, *g* was allowed to vary in many susceptibility fits cited in Table 1. *J* and *g* are positively correlated: In a fitting session a change in *g* of $+0.01$ is accompanied by a change in *J* of ≈ 1.3 cm^{-1} in the parameter space around $(g,J) \approx (2.00,200)$. This means that *J* values corresponding to high and low *g* values are over- and underestimated, respectively.

All calculations were performed on a personal computer with standard software.[32]

3. Results and Discussion

The parameter values which minimize χ^2 of eq 18 are presented in Table 2. A comparison of the calculated J_{model}

(19) Anderson, P. W. *Phys. Rev.* **1959**, *115*, 2.
(20) Glerup, J. *Acta Chem. Scand.* **1972**, *26*, 3775.
(21) Bencini, A.; Gatteschi, D. *Inorg. Chim. Acta* **1978**, *31*, 11.
(22) Atanasov, M.; Angelov, S. *Chem. Phys.* **1991**, *150*, 383.
(23) Anderson, P. W. In *Magnetism*; Rado, G. T., Suhl, H., Eds.; Academic Press: New York, 1963; Vol. 1, Chapter 2.
(24) Ginsberg, A. P. *Inorg. Chim. Acta Rev.* **1971**, *5*, 45.
(25) Schäffer, C. E. *Struct. Bonding* **1968**, *5*, 68.
(26) Kahn, O.; Briat, B. *J. Chem. Soc., Faraday Trans. 2* **1976**, *72*, 1441.
(27) Coffmann, R. E.; Buettner, G. R. *J. Phys. Chem.* **1979**, *83*, 2387.
(28) Bloch, D. *J. Phys. Chem. Solids* **1966**, *27*, 881.
(29) Shrivastava, K. N.; Jaccarino, V. *Phys. Rev. B* **1976**, *13*, 299.
(30) Ou, C. C.; Wollmann, R. G.; Hendrickson, D. N.; Potenza, J. A.; Schugar, H. J. *J. Am. Chem. Soc.* **1978**, *100*, 4717.
(31) Griffith, J. S. *The Theory of Transition Metal Ions*; Cambridge University Press: Cambridge, UK, 1961.
(32) Press, W. H.; Flannery, B. P.; Teukolsky, S. A.; Vetterling, W. T. *Numerical Recipes. The Art of Scientific Computing*; Cambridge University Press: Cambridge, UK, 1986.

Table 2. Parameter Values Obtained in the Least-Squares Fits by Using the Two Different Radial Functions Eqs 13 and 14, Columns 2 and 3, respectively

parameters	$f(r) \propto e^{-br}$	$f(r) \propto r^{-b}$
$e'_{s\sigma}$	20870	1026
$e'_{p\pi}$	20904	1143
$e'_{p\sigma}$	49815	2511
b	1.977	3.559
χ^2	9048	9054
$e_\sigma/e_\pi = (e'_{p\sigma} + e'_{s\sigma})/e'_{p\pi}$	3.4	3.1
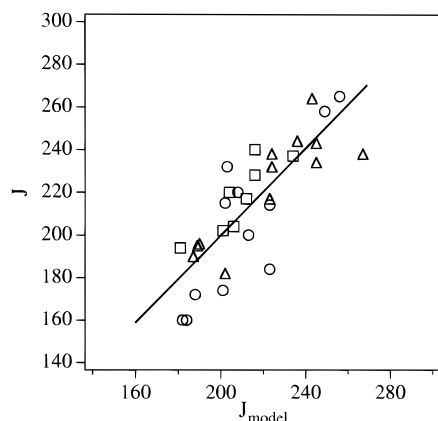
Figure 2. Plot of the experimental J values versus the model J_{model} values obtained in the least-squares fit with the radial function eq 13. The mono-, doubly- and triply-bridged dimers are represented by circles, squares, and triangles, respectively. The line $y = ax + b$ drawn is the best fit through the points ($a = 1.02$, $b = -5.4$). The regression coefficient is 0.82.

and the experimental J values is presented in Figure 2. The results with the two radial functions eqs 13 and 14 were indistinguishable. We tried to let the three types of overlaps have distinct radial dependencies, *i.e.* we introduced three b values, namely $b_{s\sigma}$, $b_{p\pi}$, and $b_{p\sigma}$. This led to meaningless results and did not improve the fits with any significance. In the absence of error bars on the experimentally determined J values we can estimate the standard deviation of J as follows.[32] If we assume that all the experimentally determined J values have the same standard deviation σ, and that the model does fit well, we can recompute σ^2 as

$$\sigma^2 = \left(\sum (J - J_{model})^2\right)/N \qquad (19)$$

where N is the number of experimental J values. We find $\sigma = 16$ cm^{-1} for both radial models. This value almost coincides with the value (21 cm^{-1}) mentioned in the previous section as an upper limit for the uncertainty of the experimental J values. Twenty three data points (72%) lie within 1σ, 8 data points (25%) in the interval 1σ to 2σ, and 1 data point (3%) in the interval 2σ to 3σ. This means that with $\sigma = 16$ cm^{-1} we have statistically accounted for the available data in a satisfactory way, because for a normal distribution the percentages would be 68%, 27%, and $\approx 5\%$.

Both radial models eqs 13 and 14 identify the pσ interaction as approximately 2.5 times stronger than the two other interactions pπ and sσ, which are comparable in magnitude (see Table 2). Kahn and Briat[26] estimated that for a linear Fe$-$O$-$Fe system the difference $|e_{s\sigma} - e_{p\sigma}|$ is similar in magnitude to $e_{p\pi}$ and that $e_{s\sigma} \approx e_{p\pi}$. Our results agree very well with these estimates.

The AOM parameter e_σ for a given ligand is given as a sum of a pσ and an sσ contribution

$$e_\sigma = e_{p\sigma} + e_{s\sigma} \qquad (20)$$

Our e_σ/e_π ratios, which are very well approximated by the e'_σ/e'_π ratios (Table 2), also agree with numerous spectroscopic studies of other oxo-coordinated species. e_σ/e_π ratios for oxide as a ligand have been found by several authors[49−51] to lie in the interval 3−6. We get values of 3.4 and 3.1 for the radial functions (13) and (14), respectively. The relative magnitudes of $e_{s\sigma}$, $e_{p\pi}$, and $e_{p\sigma}$ found here agree well with what was found in an analysis of the magnetic properties of several homo- and heteronuclear transition metal complexes containing the oxo bridge.[18]

The distance dependence of the AOM parameters is also interesting. From the radial function eq 14 we find using eq 12 and the b value from Table 2 that the AOM parameters $e_{a\alpha}$ are roughly proportional to $r^{-2b} \approx r^{-7}$. The ligand-field splitting Δ of the e$_g$ and t$_{2g}$ orbitals in an octahedral complex is defined as

$$\Delta = 3e_\sigma - 4e_\pi \qquad (21)$$

If the ligands are treated as point charges or electric dipoles, Δ is proportional to r^{-5} or r^{-6}, respectively.[52] Our r^{-7} dependence of $e_{a\alpha}$, and therefore also of Δ, is in reasonable agreement with this. An r^{-7} dependence of $e_{a\alpha}$ results in an r^{-14} dependence of J. Experimental studies[28] of other systems have indicated that J is proportional to r^{-B} with $10 < B < 12$. And a theoretical study of the V^{2+}F$^-$V^{2+} bridging geometry[29] resulted in $12 < B < 16.6$. Again we conclude that our parameters are reasonable.

In order to decide whether our four-parameter models lead to a better correlation between J_{exp} and J_{calc} than models that neglect the angle, we performed χ^2-tests.[32] $J = A \exp(-br)$

(33) Strauss, S. H.; Pawlik, M. J.; Skowyra, J.; Kennedy, J. R.; Anderson, O. P.; Startalian, K.; Dye, J. L. *Inorg. Chem.* **1987**, *26*, 724.

(34) Lippard, S. J.; Schugar, H.; Walling, C. *Inorg. Chem.* **1967**, *10*, 1825. Schugar, H.; Rossmann, G. R.; Gray, H. B. *J. Am. Chem. Soc.* **1969**, *91*, 4564.

(35) Landrum, J. T.; Grimmett, D.; Haller, K. J.; Scheidt, W. R.; Reed, C. A. *J. Am. Chem. Soc.* **1981**, *103*, 2640.

(36) Plowman, J. E.; Loehr, T. M.; Schauer, C. K.; Anderson, O. P. *Inorg. Chem.* **1984**, *23*, 3553.

(37) Mockler, G. M.; Jersey, J.; Zerner, B.; O'Connor, C. J.; Sinn, E. *J. Am. Chem. Soc.* **1983**, *105*, 1891.

(38) Coggon, P.; McPhail, A. T.; Mabbs, F. E.; McLachlan, V. N. *J. Chem. Soc. A* **1971**, 1014.

(39) Norman, R. E.; Holz, R. C.; Menage, S.; O'Connor, C. J.; Zhang, J. H.; Que, L. *Inorg. Chem.* **1990**, *29*, 4629.

(40) Hazel, R.; Jensen, K. B.; McKenzie, C. J.; Toftlund, H. *J. Chem. Soc., Dalton Trans.* **1995**, 707.

(41) Feng, X.; Bott, S. G.; Lippard, S. J. *J. Am. Chem. Soc.* **1989**, *11*, 8046.

(42) Vincent, J. B.; Huffmann, J. C.; Christou, G.; Li, Q.; Nanny, M. A.; Hendrickson, D. N.; Fong, R. H.; Fish, R. H. *J. Am. Chem. Soc.* **1988**, *110*, 6898.

(43) Armstrong, W. H.; Spool, A.; Papaefthymiou, G. C.; Frankel, R. B.; Lippard, S. J. *J. Am. Chem. Soc.* **1984**, *106*, 3653.

(44) Drüeke, S.; Wieghardt, K.; Nuber, B.; Weiss, J.; Fleischauer, H-P.; Gehring, S.; Haase, W. *J. Am. Chem. Soc.* **1989**, *111*, 8622.

(45) Hartmann, J. R.; Rardin, R. L.; Chaudhuri, P.; Pohl, K.; Wieghardt, K.; Nuber, B.; Weiss, J.; Papaefthymiou, G. C.; Frankel, R. B.; Lippard, S. J. *J. Am. Chem. Soc.* **1987**, *109*, 7387.

(46) Gomez-Romero, P.; Casan-Pastor, N.; Ben-Hussein, A.; Jameson, G. B. *J. Am. Chem. Soc.* **1988**, *110*, 1988.

(47) Adams, H.; Bailey, N. A.; Crane, J. D.; Fenton, D. E.; Latour, J-M.; Williams, J. M. *J. Chem. Soc., Dalton, Trans.* **1990**, 1727.

(48) Drüeke, S.; Wieghardt, K.; Nuber, B.; Weiss, J. *Inorg. Chem.* **1989**, *28*, 1414.

(49) Brunold, T. C.; Güdel, H. U. *Chem. Phys. Lett.* **1996**, *257*, 123.

(50) Brunold, T. C.; Güdel, H. U.; Kück, S.; Huber, G. *J. Lumin.* **1996**, *65*, 293.

(51) Lachwa, H.; Reinen, D. *Inorg. Chem.* **1989**, *28*, 1044.

(52) Schläfer, H. L.; Gliemann, G. *Einführung in die Ligandenfeldtheorie*; Akademische Verlagsgesellschaft: Frankfurt am Main, 1967, pp 344−349.
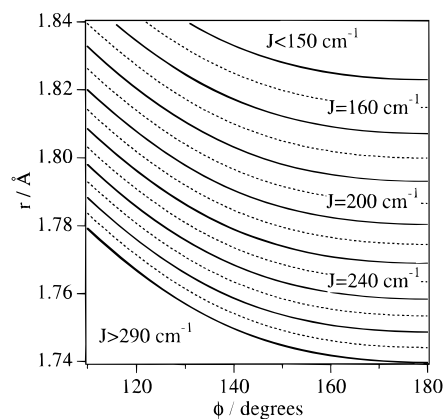
Figure 3. Angular and distance dependence of J_{model} for oxo-bridged iron(III) dimers. $r = (r_1 + r_2)/2$. The lines drawn are iso-J curves, *i.e.* they connect points with the same J_{model} value. The abscissa and ordinate axes cover the ϕ and r ranges, respectively, exhibited by the compounds in Table 1.

and $J = Ar^{-b}$ were the two-parameter model functions for the purely radial models, and the χ^2 probability function was used for the tests.[32] Values of 0.048 and 0.300 were obtained for the models excluding and including the angle dependence, respectively. On the basis of the usual criteria of statistical distributions[32] we conclude that the improvement obtained by including the angle dependence is significant.

On the basis of eq 15 and the parameter values in the first column of Table 2, corresponding to the radial function 13, we obtain by some elementary algebra the following angle and distance dependence of J_{model} (in cm^{-1}):

$$J_{model} = 1.337 \times 10^8 (3.536 + 2.488 \cos \phi + \cos^2 \phi) \times$$
$$\exp(-7.909r) \quad (22)$$

where r is the mean iron−oxide bond length (in Å) in the complex.

In Figure 3 we present the results of numerical calculations of J_{model} using eq 22 in a graphical form with r and ϕ as variable parameters. This representation allows a discussion of the r and ϕ dependencies separately.

For $\phi = 180°$ J_{model} increases from 150 to 290 cm^{-1} upon decreasing r from 1.83 to 1.74 Å. This increase of 140 cm^{-1} corresponds to approximately 9σ in eq 19. It is therefore significant, and there can be no doubt that J and r are correlated. Figure 3 shows that this is true also for smaller angles than $\phi = 180°$.

Similarly, moving horizontally in Figure 3 for a given mean Fe−O distance r we find that J_{model} increases by 60−70 cm^{-1} upon lowering ϕ from 180° to 115°. This corresponds to about 4σ, which is significant. We conclude that J and ϕ are correlated
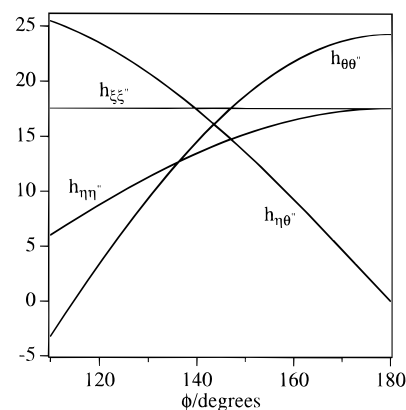

Figure 4. Angle dependency of the transfer integrals. $h''_{ab} \equiv (h^2_{ab}/U)^{1/2}$. The curves are generated by use of eqs 7−10, the parameter values in the first column of Table 2, and a mean iron−oxide distance of 1.792 Å.

with a total spread, which is about half of the r dependence. The angular dependence is somewhat less pronounced for the larger than the smaller r values. The reasons for the relatively small ϕ dependence are the competing and partially compensating electron transfers and thus exchange pathways $\eta\eta$, $\theta\theta$, $\eta\theta$ and $\theta\eta$ which maximize and minimize at different angles. From eqs 7−11 we find that $h_{\eta\eta}$ maximizes at $\phi = 180°$ and minimizes at $\phi = 90°$. $h_{\eta\theta}$ and $h_{\theta\eta}$ are zero at $\phi = 180°$ and maximize at $\phi = 90°$. $|h_{\theta\theta}|$ has yet another ϕ dependence: it maximizes at $\phi = 180°$ and 90°, and with the parameter values in Table 2 it becomes zero at $\phi = 114°$. These angle dependencies are illustrated in Figure 4. We note that the increase of J with decreasing bridging angle ϕ is in contrast to the decrease proposed in refs 10 and 11. On the other hand, it is in agreement with the results of a more recent *ab initio* study of $Cl_3Fe−O−FeCl_3{}^{2-}$).[15]

In conclusion, we have accounted for the dependence of the antiferromagnetic exchange parameter J on the Fe−O−Fe angle and the Fe−O distances in μ-oxo-bridged iron(III) dimers by using an angular and radial overlap model. To our knowledge this work represents the first attempt to extract several angular overlap model parameters solely from magnetic susceptibility data. The angular overlap model parameters for oxide as ligand on iron(III) were found to have the approximate relative ratios $e_{p\sigma}:e_{p\pi}:e_{s\sigma} \approx 2.5:1:1$.

The model presented here can easily be extended and modified to account for the magnetic properties of other dinuclear complexes with one oxo bridge.[18]